

www.acsami.org Research Article

Liquid-Infused Membranes Exhibit Stable Flux and Fouling Resistance

Rushabh M. Shah, Aydın Cihanoğlu, Justin Hardcastle, Caitlin Howell, and Jessica D. Schiffman*



Cite This: ACS Appl. Mater. Interfaces 2022, 14, 6148–6156



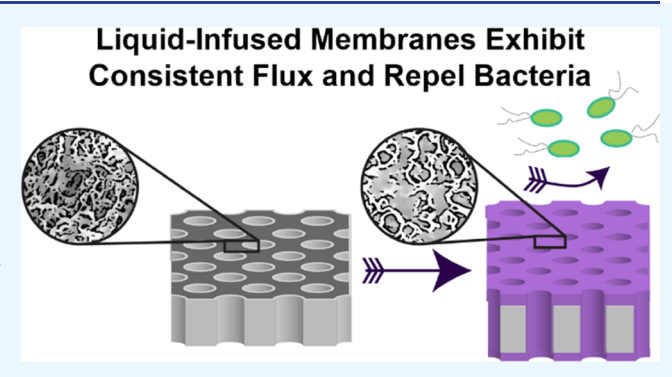
ACCESS

Metrics & More



SI Supporting Information

ABSTRACT: Antifouling membranes that offer excellent operational lifetimes are critical technologies needed to meet the growing demand for clean water. In this study, we demonstrate antifouling membranes featuring an ultrathin oil layer that stayed immobilized on the surface and in the pore walls of poly(vinylidene fluoride) membranes for multiple cycles of operation at industrially relevant transmembrane pressures. An optimized quantity of a commercial Krytox oil with either a low (K103) or a high viscosity (K107) was infused onto the active surface and into the pores of membranes with a 0.45 μm pore size. The presence of the oil layer was qualitatively confirmed using crystal violet staining and variable pressure scanning electron microscopy. Using a dead-end stirred cell, a consistent pure water permeance value of 3000 L m $^{-2}$ h $^{-1}$



bar $^{-1}$ was achieved for the K103 liquid-infused membranes for at least 10 operation cycles, which was expectedly lower than the permeance of bare control membranes (\sim 16 000 L m $^{-2}$ h $^{-1}$ bar $^{-1}$), suggesting that a stable oil layer was formed on all membrane-active sites. To quantify if oil was lost during membrane operation, extensive thermogravimetric analysis was conducted on both the as-prepared and used membranes. When challenged with the microorganism, *Escherichia coli* K12, the liquid-infused membranes statistically reduced microbial attachment by \sim 50% versus the control membranes. For the first time, we have demonstrated that by forming an immobilized, robust, and stable oil-coated membrane, we can generate high-performance membranes with stable permeance values that can be operated at relevant transmembrane pressures and provide long-lasting antifouling properties.

KEYWORDS: antifouling, bioinspired, Escherichia coli, flux, membranes, ultrafiltration

■ INTRODUCTION

Degrading water quality is a persistent problem, which is corroborated by the fact that globally, 2.2 billion people lack access to clean drinking water. $^{\rm I,2}$ The World Economic Forum has declared that the water crisis is a societal and environmental risk leading to the transmission of diseases, including diarrhea, cholera, typhoid, and hepatitis A.3 One in nine children under the age of five die every day due to diarrhea making diarrhea the second leading cause of childhood mortalities worldwide. 4-6 To fight this water paucity and degrading water quality, membrane-based water treatment processes, including ultrafiltration, are used because membrane-based technologies can effectively remove the particulates and pathogens (viruses and bacteria) that cause waterborne diseases. However, over time biofouling, i.e., the accumulation of particulates and pathogens on the membrane and inside their pores, contributes to more than 45% of all membrane fouling,8 as well as causes an increase in energy consumption and a decreased rate of clean water production.

Various strategies to reduce biofouling during membrane operation have previously been explored, including both operational changes and altering membrane design. For example, researchers have investigated how both physical methods (i.e., flow-induced shear, ^{10,11} gas sparging ^{12,13}) and chemical methods (i.e., feed stream pretreatment ¹⁴) can decrease biofouling during membrane operation. However, these approaches have their own shortcomings. For example, flow-induced shear causes the breakage of foulant particles that lead to pore blocking. ¹¹ In terms of re-engineering the design of membranes via the inclusion of functional chemistries, a popular approach has been to blend active agents, such as biocides ^{15–17} and/or antifouling polymers ^{18–21} into the body of the membrane. While this approach can effectively decrease biofouling, it is often accompanied by a trade-off in membrane performance. ^{22,23} Another drawback is that the bioactive moieties are located throughout the membrane as opposed to the interfacial location that is actively involved with the

Received: October 26, 2021 Accepted: January 6, 2022 Published: January 19, 2022





separation, and thus, higher loadings are required for activity.²⁴ While modifying membrane surfaces with antimicrobials (e.g., metal ions, titanium dioxide^{25–27}) and/or antifouling polymers (i.e., zwitterions, poly(ethylene glycol)^{28–30}) can effectively concentrate active agents at the surface of the membrane, complicated reaction chemistries or manufacturing, including chemical grafting, plasma treatments, and/or UV treatments, are typically required. This impedes industrial scale up and prevents fouling only on the membrane's surface rather than within the membrane's pores.^{31–35} Thus, an alternative, straightforward approach that transforms all membrane-active sites, including, the surface skin and pores to be fouling resistant without compromising consistent separation performance, is needed.

In nature, the Nepenthes pitcher plant uses a thin, immobilized liquid layer to create an ultraslippery surface, which causes insects to slide down into its cup. 36 To mimic this behavior, liquid layers have been immobilized on the surface of highly wettable microstructures, creating a pressurestable, omniphobic antifouling coating on solid surfaces, commonly known as slippery liquid-infused porous surfaces (SLIPS).³⁷ SLIPS have been reported to repel a wide range of contaminants, including crude oil,³⁷ proteins,^{38,39} blood,^{38,40} and bacteria. 41,42 Inspired by this work, Hou et al. 43 demonstrated that a fluorinated lubricating oil could be infused into filters with 0.2 μ m, 5.0 μ m, and 20.0 μ m pore size that were composed of the synthetic fluoropolymer, polytetrafluoroethylene, $(C_2F_4)_n$. At ambient pressure (i.e., a gauge pressure of 0 bar), the liquid filled the 5.0 μ m pores. When a threshold pressure of 0.33 bar was applied, the liquid was stabilized by capillary forces within the 5.0 μ m pores creating a nonfouling, liquid-lined pore. The threshold pressure required to allow liquid passage through the pores depended on the size, geometry, and composition of the bare membrane, as well as the surface tension of the lubricating liquid. 43,45 In a 2021 report by Bazyar et al. 46 it was demonstrated that liquid-infused membranes have great potential at decreasing biofouling during long-term cross-flow experiments. Despite these promising preliminary investigations, to date there have been no reports that investigate if the composite membranes can perform liquid separations at industrially relevant transmembrane pressures or that quantify the stability of the oil layer after membrane operation.

Here, we report the fabrication of liquid-infused membranes (LIMs) that provide consistent pure water flux at industrially relevant transmembrane pressures. Using two nontoxic, chemically inert, omniphobic perfluoropolyether liquids with varying viscosities, we were able to confirm the formation of a stable liquid layer on the surface and in the pores of commercial poly(vinylidene fluoride) (i.e., $(C_2H_2F_2)_n$) membranes. We tested the pure water permeance of these liquid-infused membranes with varying pressure, resting time, and over ten testing cycles using a dead-end filtration unit. The highly antifouling properties of these composite membranes were also demonstrated.

MATERIALS AND METHODS

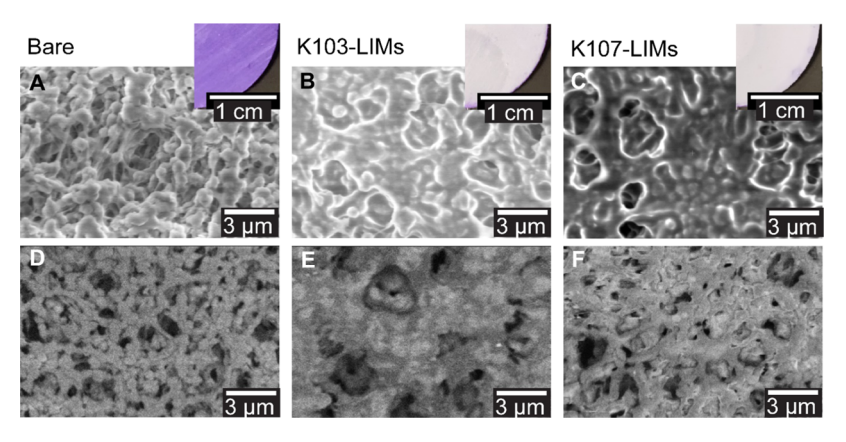
Materials and Chemicals. Perfluoropolyether Krytox 103 (K103) with a low viscosity of 0.000082 m 2 s $^{-1}$ (82 cSt) and perfluoropolyether Krytox 107 (K107) with a higher viscosity of 0.001535 m 2 s $^{-1}$ (1535 cSt) were purchased from Chemours (Wilmington, DE). Isopropyl alcohol (IPA, 70% v/v) was purchased from ThermoFisher Scientific (Waltham, MA). ACS reagent grade

acetone was purchased from Fisher Scientific (Hampton, NH). Deionized (DI) water was obtained from a Barnstead Nanopure Infinity water purification system (resistance of 18.2 M Ω cm, ThermoFisher Scientific). Luria-Bertani broth (LB), M9 minimal salts (M9 media), sodium chloride (NaCl), D-(+)-glucose, carbenicillin (BioReagent grade), and crystal violet (ACS reagent, >90%, anhydrous basis) were purchased from Sigma-Aldrich (St. Louis, MO).

Fabrication of Liquid-Infused Membranes (LIMs). Poly-(vinylidene fluoride) (PVDF) membranes with a reported pore size of 0.45 μm were purchased from ThermoFisher Scientific and used in all studies. Prior to use, a flushing procedure was conducted to remove glycerol from the membrane's pores. Membranes were submerged in a 70% IPA for 0.5 h before being rinsed with DI water three times. All flushed membranes were stored in DI water at 4 °C until use. To prepare the liquid-infused membranes (LIMs), 6 μ L cm $^{-2}$ of K103 or 15 μL cm $^{-2}$ of K107 was applied to the surface of a flushed and compacted membrane using a micropipette. The previously mentioned quantities of Krytox were systematically optimized, as discussed in the results sections. The liquid was allowed to spread across the membrane surface and into the pores for 30 min. Membranes were next suspended vertically for 60 min to allow the excess lubricant to runoff the membrane due to gravitational forces. No additional forces or pressures were applied during the membrane fabrication process. Throughout this article, the composite membranes coated with Krytox 103 or Krytox 107 are referred to as K103-LIM and K107-LIM, respectively. The flushed PVDF membranes that were used as controls (without a lubricating liquid layer) will be referred to as the bare membrane.

Characterization of LIMs. Variable pressure scanning electron microscopy (VP-SEM, ThermoFisher VolumeScope V2), with an acceleration voltage of 5 kV and a variable pressure of 0.38 torr, was used to characterize the surface morphology of both the bare membranes and LIMs. Images were captured in Secondary Electrons (SE, 15 pA) and BackScatter (BS, 400 pA) imaging modes. To qualitatively confirm the presence of the lubricant layer, crystal violet was applied to wet LIMs because as an aqueous stain, it can only stain portions of the membranes that lack the lubricant. LIMs and bare membranes were submerged in 1.5 mL of 0.001% aqueous crystal violet stain that was agitated at 90 rpm using a MaxQ2000 (ThermoFisher Scientific) for 20 min. Digital images of the membranes were captured using a OnePlus 6t 16 + 20 MegaPixel camera. Static contact angle measurements were acquired using 10 μ L drops of DI water on the bare membranes using a Canon EOS 6D Mark II camera with a 100 mm macro lens (Canon, Huntington, NY). Tilt contact angle measurements were performed by placing a 25 μ L DI water droplet on one side of the bare membrane or LIM, which was placed on an AP180-Adjustable Angle Mounting Plate (Thorlabs, Newton, NJ) equipped with an AccuMaster digital level/angle gauge (Carson, NV). The stage was slowly tilted until the water droplet started to move. Between each tilt angle measurement, the membrane was rotated by 45° to ensure that no water droplet moved along the same path twice. If no droplet movement occurred before 45°, the measurement was declared a failure. The reported static contact angles and tilt angles are the averages of 12 drops acquired over 4 different samples.

Performance of LIMs. Pure water permeance experiments were conducted using a 10 mL dead-end stirred cell (Sterlitech, Kent, MA). The membrane-active area was 3.8 cm². The dead-end stirred cell was pressurized using a nitrogen (N_2) tank and the flux was calculated by measuring the change of mass on the permeate side using a digital weighing scale (U.S. Solid, Cleveland, OH). All of the pressure values reported throughout this article are the gauge pressure values. First, each flushed bare membrane was compacted for 0.5 h at 3 bar pressure, which ensured that the flux change was less than 5%. Next, permeance tests on the LIMs were performed for 0.5 h at four different transmembrane pressures (TMPs = 1, 2, 3, and 4 bar). Flux as a function of the volume of water that permeated through the membrane (ΔV), membrane area (A), and time (Δt) was calculated



www.acsami.org

Figure 1. VP-SEM micrographs acquired using (A-C) secondary electrons and (D-F) backscatter modes. Micrographs of (A, D) bare, (B, E) K103-LIMs, and (C, F) K107-LIMs are provided. Crystal violet stained membranes are provided in the inset digital images and additional digital images are provided in Figure S1.

using eq 1, whereas pure water permeance and normalized permeance were determined using eqs 2 and 3, respectively.

flux (L m⁻² h⁻¹) =
$$\frac{\Delta V}{A\Delta t}$$
 (1)

$$permeance (L m-2 h-1 bar-1) = \frac{flux}{TMP}$$
 (2)

normalized permeance
$$\left(\frac{PWP}{PWP_0}\right)$$

$$= \frac{\text{pure water permeance of LIMs}}{\text{pure water permeance of bare membrane}}$$
(3)

The effect of resting time on the long-term pure water permeance of the LIMs was explored. Five filtration cycles, which were each 30 min in duration, were performed on the same LIM at 1.5 bar TMP. After each cycle of pure water flow, the LIMs were allowed to rest for 15 or 30 min, i.e., they remained undisturbed in the dead-end stirred cell with no pressure gradient, washing, or another contact. The LIM remained in the dead-end cell for all 5 testing cycles and no additional Krytox was added to the system. The same water was used for all 5 cycles of a resting time experiment.

Continuous long-term permeance experiments were also conducted on the LIMs. Ten filtration cycles (30 min each) were performed on the same LIM sample at 1.5 bar TMP. There was no resting time (0 min) between the continuous testing cycles. The membrane sample being tested remained in the dead-end stirred cell for the entire duration of the ten cycles of testing. No additional Krytox was added to the system. The same water was used for all 10 cycles of the long-term experiment.

Thermogravimetric analysis (TGA, Q50, TA Instruments) was conducted to determine the percentage of Krytox that remained on the as-prepared and used LIMs (post-permeance experiments). A membrane sample (6–12 mg) loaded onto a platinum pan was heated from 25 °C to 700 °C at a temperature ramp of 10 °C min⁻¹. The nitrogen was purged at a flow rate of 40 mL min⁻¹ for the balance and 60 mL min⁻¹ for the sample. The ratio of Krytox to the commercial membrane was determined using the TGA data provided in Table S1 and using eq 4

$$K/M \text{ ratio} = \frac{K \text{rytox (\%)}}{\text{bare membrane (\%)}}$$
(4)

Antifouling Activity of LIMs. Bacteria antifouling tests were conducted as reported previously 47 using Escherichia coli K12 MG1655 (E. coli), a Gram-negative strain purchased from DSMZ, Leibniz-Institut, Germany, containing a green fluorescent protein (GFP) plasmid. Control glass coverslips (22 mm × 22 mm, Fisher Scientific, Hampton, NH) were cleaned by submerging them in an acetone bath (stirred at 60 rpm) for 10 min followed by rinsing with

autoclaved DI water three times, before being dried at 60 °C for 16 h and treated with UV/ozone (ProCleanerTM, Bioforce Nanosciences, Ames, IA) for 10 min. Both sides of the bare membranes (circular coupons with 2.54 cm diameters) were sterilized using a UV lamp (UVP UVGL-58, Analytik Jena US, Upland, CA) for 10 min. K103 and K107 oils were sterilized by passing them through a sterile vacuum filter of 0.45 μm pore size (Stericup Quick Release, EMD Millipore Corporation, Billerica, MA). After sterilization, the bare membranes were coated with sterilized K103 or K107 to fabricate the LIMs, as described previously. E. coli was inoculated with 100 μg mL⁻¹ carbenicillin and grown overnight in LB media at 37 °C to a concentration of 108 cells mL⁻¹. All membrane samples were placed at the base of six-well plates (Fisher Scientific) to which 5 mL of M9 media containing 250 µL of E. coli was added to each of the six wells and placed in an incubator at 37 °C for 2 h. Membrane samples were then removed from the six-well plates and gently rinsed with M9 to remove the loosely adherent bacteria. At least 15 random images of the samples with adhered microbes were acquired using two parallel replicates on three different days using an Axio Imager A2M microscope (20 × magnification, Zeiss, Thornwood, NY). Bacteria colony area coverage (%) was calculated using the particle analysis function in ImageJ 1.53a software, 48 consistent with our previous work.4

Statistics. For all of the data, an unpaired Student's t-test was used to determine the statistically significant difference between samples. Significance is denoted in the graphs using asterisks (*) and defined in figure captions. All experiments were conducted in triplicate.

■ RESULTS AND DISCUSSION

Characteristics of Liquid-Infused Membranes (LIMs).

The goal of this work was to create a continuous and stable lubricant layer in the pores and on the surface of membranes to test the hypothesis that liquid infusion could provide a novel route to enhancing the fouling resistance of high-performance membranes. Commercial poly(vinylidene fluoride) (PVDF) membranes were selected to serve as the base membranes because of their chemical affinity for the perfluoropolyether liquid that results from the presence of fluorine groups,³⁷ their durability, and because they are commonly used in the separation industry. While a Magellan 400 XHR scanning electron microscope (FEI, Hillsboro, OR) was able to capture images of the control bare membrane, images could not be acquired after the application of the oil. Thus, in Figure 1, we present VP-SEM micrographs for all membrane samples; due to the combination of elevated gas pressures within the sample chamber and specialized electron detectors, 50 it was possible to image both bare membranes and those featuring an

immobilized liquid. The bare membranes display a polydispersed pore-size distribution (Figure 1A) and a fibrous-like structure with interconnected pores was also observed.

We successfully fabricated liquid-infused membranes (LIMs) using PVDF membranes as the base and the perfluoropolyether oil, Krytox 103 or 107 having a low viscosity of 0.000082 m² s⁻¹ (82 cSt) or a high viscosity of $0.001535 \text{ m}^2 \text{ s}^{-1}$ (1535 cSt), as the infusion lubricant. The quantity of K103 or K107 that needed to be applied to the surface of the membranes was selected based on the previous literature 45 and further optimized by systematic investigations. Visually, we added sufficient lubricating oil so that it could be evenly spread over the entire surface of the membrane and the surface appeared shiny to the unaided eye. All membranes coated with the oil were held vertically for 60 min, which allowed any excess liquid to runoff the membrane. In the case of both oils, the quantity was lower (6 μ L cm⁻² for K103 and 15 μ L cm⁻² for K107) than that reported in the literature (250 μ L cm⁻²) potentially due to differences in pore size and/or geometry of the base materials.⁴⁴ Because the K107 has a higher viscosity than K103, a greater quantity of K107 was required to spread evenly over the membranes, which was expected.

Due to the membrane pore-size distribution being polydisperse, reporting an average pore diameter of either the bare membranes or the LIMs was not a reliable characteristic of the membrane. However, micrographs acquired on LIMs using secondary electron imaging display that the immobilized oils visually appeared to have generally decreased the pore diameters (see Figure 1B,C). When using the backscatter mode, the LIMs (Figure 1E,F) had an enhanced bright field compositional contrast compared to the bare membranes (Figure 1D) due to the presence of additional fluorine groups in the oil. This was also expected because the densities of the oils $(K103 = 1.92 \text{ g cm}^{-3} \text{ and})$ $K107 = 1.95 \text{ g cm}^{-3}$) are greater than those of the PVDF membranes (1.78 g cm⁻³), thus increasing the bright contrast of the LIMs versus the bare membranes. Because the backscatter imaging mode uses a higher current, the electrons also penetrate into the membrane's body and down into the pores; this increased penetration depth results in the increased contrast and suggests the presence of oil inside the membranes.

We next used a qualitative method to confirm that the lubricating oil coated the entire membrane surface. We submerged the LIMs into the aqueous crystal violet stain 44,51 that would not be able to dye the perfluoropolyether lubricant oils. As shown in the inset image in Figure 1A, the bare PVDF membrane was fully stained purple, whereas the K103- and K107-LIMs both retained their original white color (see also Figures 1B,C and S1), thereby strongly suggesting the presence of Krytox on the membrane's surface.

The hydrophobicity of the bare membranes was determined using static water contact angle measurements (Table S2). The bare membranes had a hydrophobic contact angle of $115 \pm 8^{\circ}$, consistent with literature values. ⁵² We did not provide static contact angles for LIMs because it has been reported to be an unreliable measurement; the oil layer can wrap around the water droplet giving a false contact angle measurement. ^{43,44} Thus, tilt contact angle measurements were acquired for the LIMs and bare membranes to examine the continuity and functionality of the liquid layer. ^{53,54} Table S2 displays that no water droplet movement was observed on the bare membranes before a tilt angle of 45° , whereas immediately after applying

the oil, the LIMs displayed a statistically lower tilt angle of 9° (see Table S3). As part of our procedure to produce the LIMs, they are held vertically for 60 min to remove any extra oil from the membranes; on the LIMs where the excess oil was allowed to runoff the sample, we observed a tilt angle of $37 \pm 7^{\circ}$ and a statistically lower angle of $19 \pm 8^{\circ}$ for K103- and K107-LIMs, respectively. Potentially, the K107-LIMs had a lower tilt angle than the K103-LIMs because of the oil's higher viscosity and surface tension that might lead to a greater volume of oil being retained on the surface. Overall, these decreased tilt angles further confirm the presence of the slippery lubricant layer on the membranes, i.e., the presence of an oil layer that enables the sliding of a water droplet to occur at a lower tilt angle.

Pure Water Permeance of LIMs as a Function of Transmembrane Pressure (TMP). Next, we investigated the ability of LIMs to be used in high-pressure systems. First, we determined the optimal transmembrane pressure (TMP) to carry out long-term experiments by performing pure water permeance experiments as a function of TMP (i.e., 1, 2, 3, and 4 bar). The dotted line in Figure 2 represents the permeance of

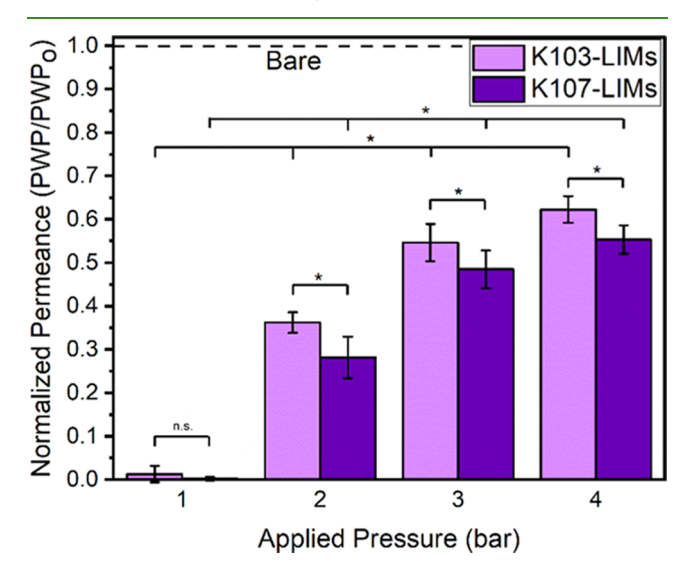


Figure 2. Normalized permeance for K103-LIMs and K107-LIMs as a function of transmembrane pressure (TMP). The dotted line represents the normalized permeance of the bare membranes. Error bars denote standard deviation, one asterisk (*) denotes a $p \leq 0.05$ significance between samples, and n.s. denotes that samples were not statistically different.

the bare (noninfused) membrane, against which, we normalized our LIM data. As expected, all permeance values for LIMs were statistically lower than those for the bare PVDF membranes, even at the highest TMP of 4 bar (the limit of our dead-end stirred cell). This immediately indicates that lubricant is retained in/on the membranes after testing at all TMPs used in this work. We expected our LIMs to have a lower flux than those of the bare membranes.

At the lowest TMP (1 bar), K103-LIMs and K107-LIMs both exhibited a very low permeance, close to zero. After increasing the TMP from 1 bar to 2 bar, a statistically significant increase in the normalized permeance (see eq 3) was observed for the K103- and K107-LIMs. This is likely because a threshold TMP was reached between 1 and 2 bar, resulting in potentially the opening of the pores if they were clogged with the oil or simply an allowance of the water to pass through oil-decorated pores. Increasing the operating pressure

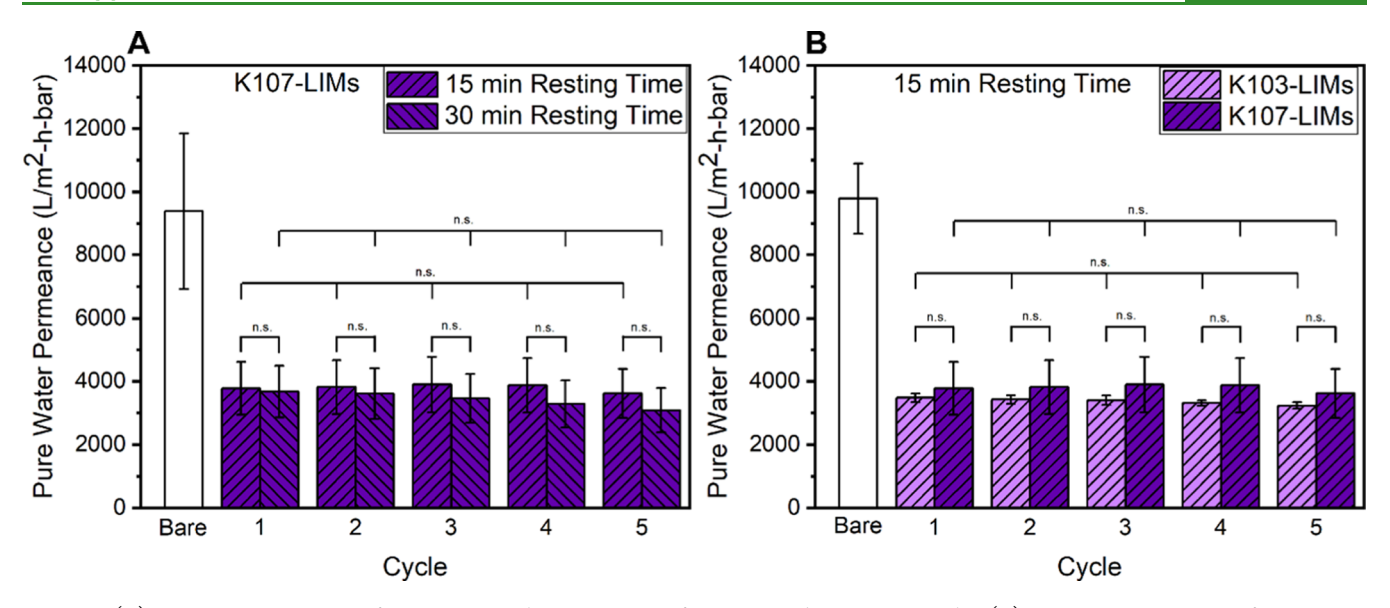


Figure 3. (A) Pure water permeance of K107-LIMs with 15 or 30 min of resting time between test cycles. (B) Pure water permeance of K103-LIMs and K107-LIMs with a 15 min resting time between testing cycles. A TMP of 1.5 bar was used. Error bars denote standard deviation, and n.s. denotes that samples were not statistically different. The initial pure water permeance of compacted bare membranes is provided as a comparison and is statistically different from the LIMs.

to 2 bar also revealed that the viscosity of lubricant oil yielded a statistically different LIM permeance. To better understand this threshold, we also performed pure water permeance experiments at TMPs of 1.3 bar and 1.5 bar and saw a statistical increase from 1 to 1.3, as well as from 1.3 to 1.5 bar for the K103-LIMs (see Table S4 and Figure S2). We report no statistically significant increase between 1.5 and 2 bar TMP.

Figure 2 displays that additional increases were observed for the LIMs operated at 2 versus 3 versus 4 bar TMP. For example, the normalized permeance of the K103-LIMs statistically increased to 0.55 and 0.62, whereas the normalized permeance of the K107-LIMs increased to 0.49 and 0.55 at TMPs of 3 and 4 bar, respectively. The K103-LIMs exhibited a 12% greater increase in the normalized permeance than the K107-LIMs at 4 bar. One possible explanation for this difference is that the higher-viscosity lubricant fills more volume of the membrane's pores.

These results demonstrate that LIMs provide consistent flux and suggest the presence of a stable lubricant layer for a 30 min testing duration. Based on these results, the long-term experiments in the following sections use 1.5 bar TMP because we consider 1.5 bar as the threshold pressure whereupon we report the onset of increased water permeance. In other words, while an increase in pure water permeance was observed at higher applied pressures, it is preferable to operate at the lowest threshold pressure to conserve energy.

Long-Term Pure Water Permeance of LIMs as a Function of Resting Time. Previous literature published by researchers working with liquid-infused filters reported the use of "resting time", i.e., the time required for the system to refill with oil, which assists in passive flux recovery. 43,44 To determine if incorporating a resting time would impact the flux behavior of our LIMs, we performed five permeance experiments at TMP of 1.5 bar, and after each cycle, the LIMs were allowed to "rest" in the system (no applied pressure) for 15 or 30 min, as provided in Figure 3A. Interestingly, counter to what has been reported in the literature, K107-LIMs with 15 and 30 min resting time exhibited a statistically equivalent

permeance for each cycle and as expected a lower permeance than the bare membranes.

Because there were no statistically relevant permeance differences with 15 and 30 min resting time, we next performed pure water permeance experiments using K103-LIMs with the lower resting time, i.e., 15 min, and compared the values with that of K107-LIMs. We again observed statistically equivalent permeance for the low- and high-viscosity oil-infused membranes (Figure 3B), proving that we see no effect of resting time on the permeance values at a TMP of 1.5 bar. The pure water permeances for K103-LIMs after 1 cycle and 5 cycles were 3476 ± 135 and 3230 ± 104 L m⁻² h⁻¹ bar⁻¹, respectively, and for K107-LIMs, pure water permeances of 3777 ± 836 and 3623 ± 780 L m⁻² h⁻¹ bar⁻¹ were reported.

The results in Figure 3B inform us that the permeance values at 1.5 bar TMP do not depend on the lubricant viscosity as equivalent pure water permeances were observed. Again, the resting time had no effect on the permeance. While we, like the literature, note that there was a threshold pressure required to open the pores^{43,45} or achieve an initial flux, in our higherpressure system, we hypothesize that once the oil-coated pores allow for the passage of water, they do not refill, and hence, a "gating" mechanism was not observed for our system. What is meant by a gating mechanism is that on applying pressure the liquid is pressed against the pore walls allowing the filtration liquid to pass and when this pressure is released, the pores get refilled by the liquid. 43 While a high-viscosity lubricant and 30 min resting time improved the performance of a liquid-infused system operated at a low pressure of ~ 0.7 bar, ⁴⁴ we have a very stable system at all applied pressures. In fact, without the presence of a gating mechanism, the resting time has no effect on the permeance, and thus, we can operate our system continuously. The statistically equivalent permeance suggests that little to no oil is leaving the system; this is further analyzed and discussed in the following sections. Notably, our data suggests that the mechanism of this system is fundamentally different from the gating mechanism previously published in the literature.

Continuously Operated, Long-Term Pure Water Permeance of LIMs. With the knowledge that resting time does not impact permeance, 10 cycles of pure water permeance experiments were performed continuously, without any resting time (see Figure 4). For K103-LIMs, over 10 testing cycles, we

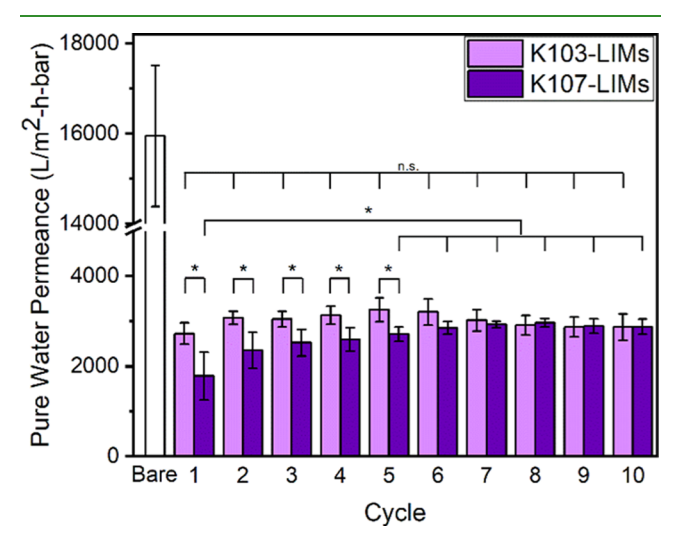


Figure 4. Pure water permeance of K103-LIMs and K107-LIMs for 10 consecutive cycles. A TMP of 1.5 bar was used. Error bars denote standard deviation, one asterisk (*) denotes a $p \le 0.05$ significance between samples, and n.s. denotes that samples were not statistically different. The initial pure water permeance of compacted bare membranes is provided as a comparison and is statistically different from the LIMs.

see a consistent permeance of ~3000 L m⁻² h⁻¹ bar⁻¹. This promising result suggests that very little to no oil is leaving the system and that the same amount of water is flowing per unit time, per unit area, and per bar pressure. If oil was being removed from the membranes, then the flux would dramatically increase, likely to the permeance values demonstrated by the bare membrane (~16000 L m⁻² h⁻¹ bar⁻¹). In all cases, the permeance for both K103- and K107-LIMs was lower than the permeance of bare membranes confirming the presence of the oil in the membrane pores. In the case of K107-LIMs, we observed an increase in the permeance value until cycle 5 and consistent permeance values from cycle 5 onward. Additionally, the pure water permeance value for cycle 1 was statistically different from the pure water permeances for cycle 5 to cycle 10. Potentially, this behavior resulted because the higher-viscosity lubricant takes a longer time to form a steady membrane pore coating when we operate the system at 1.5 bar TMP. Once a steady membrane pore coating was formed, a stable flux of \sim 2900 L m⁻² h⁻¹ bar⁻¹ was observed for cycles 5-10. Due to the significant amount of time required for these long-term tests, we did not test more than 10 cycles. However, based on these results, we suggest that performing even longer-term pure water permeance tests, i.e., more than 10 test cycles, would indeed be possible.

Lubricant Stability Using Thermogravimetric Analysis After Pure Water Permeance Experiments. We performed thermogravimetric analysis (TGA) to quantify the amount of K103 and K107 present in the as-prepared membranes and the LIMs used in pure water permeance tests (Figure S3). We used eq 4 to calculate the proportion of Krytox to the bare membrane. The weight percentage of Krytox for the as-prepared K103- and K107-LIMs was 44 ± 5

and 41 \pm 6%, respectively. Table S1 contains both the weight percentage of Krytox and the K/M ratio for the LIMs. We determined that the K/M ratio for the K103-LIMs was greater than 1, whereas for K107-LIMs, it was less than 1. This means that the weight of K103 was more than the weight of the bare membrane, whereas in the case of K107, it was less than the weight of the bare membrane. For K103-LIMs, the K/M ratio dropped significantly from 1.19 \pm 0.39 for the as-prepared membranes to 0.45 \pm 0.16 for membranes used in one permeance test, i.e., 0.8 mg cm⁻² of K103 was removed (Figure 5). Importantly, there was no significant difference, i.e., no

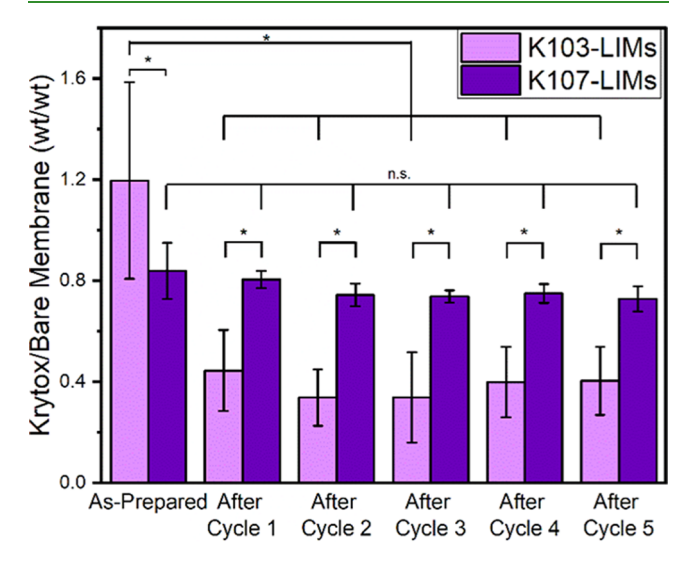


Figure 5. Krytox/Bare membrane (K/M ratio) for as-prepared and used K103-LIMs and K107-LIMs after pure water permeance testing at 1.5 bar TMP. The K/M ratio was calculated using the TGA data from Table S1 and eq 4. Error bars denote standard error, one asterisk (*) denotes a $p \le 0.05$ significance between samples, and n.s. denotes that samples were not statistically different.

weight change from cycle 1 to cycle 5 for the K103-LIMs. The pure water permeance data (Figure 4) and TGA data (Figure 5) support the hypothesis that K103 reached a steady-state concentration after one cycle of use and retained a consistent permeance over the next 9 cycles. This would only be possible if the oil remained on the membrane as a stable layer.

Since all detectable K103 losses occurred after cycle 1, we suggest that using a membrane pretreatment procedure like forward flushing, pulling pressure during membrane fabrication, or washing the membrane surface could be performed to overcome this limitation. Notably, membrane pretreatment (i.e., flushing) is very common. Additionally, further optimizations to the initial quantity of oil being applied to the membrane and/or the duration of the step where we hold the membrane vertically to allow the excess oil to runoff during the fabrication step can be optimized to minimize excess lubricant. Alternatively, if the Krytox oil was initially applied to the membranes using an industrial coating process (i.e., not via hand pipetting), it should be possible to achieve a thinner layer of oil.

For the K107-LIMs, the K/M ratio of the as-prepared membranes was statistically equivalent to the K/M ratio of the used membranes from cycles 1 to 5 of the permeance tests. Potentially, these phenomena were observed due to the higher viscosity of K107. In the case of K107-LIMs, potentially less oil can enter the membrane's pores due to its higher viscosity and

more oil drips off during the membrane preparation step. However, the oil that goes into the pores is very stable at 1.5 bar TMP, and thus, the normalized values are equivalent. A stable liquid infusion is fabricated even before applying pressure, and thus, we see no change in the K/M ratio for the K107-LIMs.

Bacterial Antifouling Activity of LIMs. The resistance to bacterial fouling was determined for the LIMs and compared to the bare membranes using *E. coli*. Statistically, fewer *E. coli* attached to the K103- and K107-LIMs than to the bare membranes (see Figure 6). In comparison to the bare

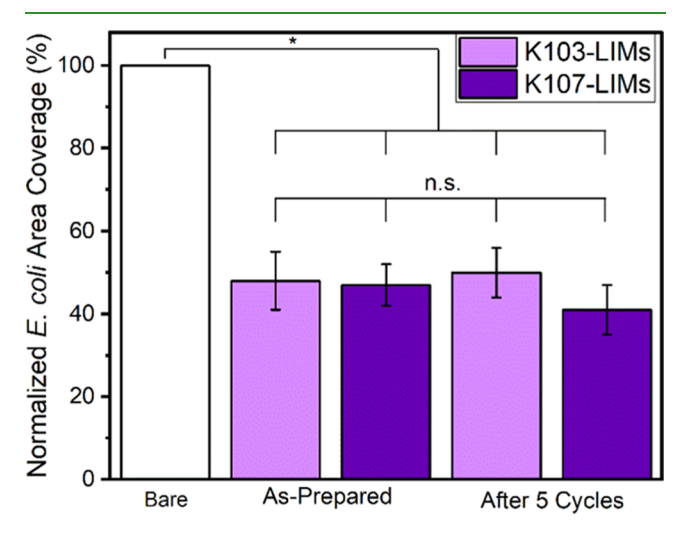


Figure 6. Area coverage of *E. coli* after 2 h incubation on bare, as well as as-prepared and used K103-LIMs and K107-LIMs after pure water permeance testing at 1.5 bar TMP. Error bars denote standard error, one asterisk (*) denotes a $p \le 0.01$ significance between samples, and n.s. denotes that samples were not statistically different.

membranes, E. coli attachment decreased by more than 50%, to 48 \pm 7% and to 47 \pm 5% for K103-LIMs and K107-LIMs, respectively. Glass coverslips were run as an internal control (data not shown) and fouled significantly more than any of the membranes. Looking to the literature, SLIPS fabricated by immobilizing perfluoropolyether (K100 and K103) liquids on PTFE supports showed a reduction in biofilm coverage of E. coli by 96% and Staphylococcus aureus by 97.2%. 41 The previous work on liquid-infused surfaces features the gating mechanism, which implies that the oil is moving; during this oil movement, it has been postulated that the bacteria are being pulled off along with the nonstable liquid coating. 44 Due to our uniquely stable oil-coated membranes, a direct comparison between our data on initial adhesion and the published data on biofilm formation is challenging. At the same time, our results are excellent and expected because the lubricant coating is slippery, which makes it difficult for bacteria to adhere.

We also performed an assay that quantified the $E.\ coli$ attachment to the LIMs after performing 5 cycles of pure water permeance experiments. $E.\ coli$ attachment again decreased significantly compared to the bare membranes to 50 ± 6 and $41\pm 6\%$ for the used K103-LIMs and K107-LIMs, respectively. In fact, a statistically equivalent antifouling performance was demonstrated by both the as-prepared LIMs and the LIMs after 5 cycles of use. Our results demonstrate that LIMs are highly repellant to the microorganism $E.\ coli$, even after using them for pure water permeance experiments. The improvement in bacterial

antifouling capabilities, especially for the used K103- and K107-LIMs, reinforces that a continuous, stable lubricant coating was formed and maintained. It is remarkable that we observed no change in the bacterial adhesion after 5 cycles of using the LIMs even though a small amount of K103 lubricant oil is removed during the pure water permeance experiments (as suggested by the TGA data). Thus, our results strongly support that ample Krytox remains on the surface of the membranes after their long-term use for both continued membrane function and antifouling properties. In this work, we have demonstrated the fabrication of LIMs that have a continuous immobilized lubricant coating, great membrane flux, and effective antifouling properties.

CONCLUSIONS

For the first time, we have demonstrated that by immobilizing an immiscible liquid to the surface and in the pores of a membrane, we can transform a membrane to provide consistent long-term flux at industrially relevant TMPs that are repellant to microorganisms. The formation of a stable lubricant layer within the membrane pores was evident because the LIMs exhibited a statistically lower pure water flux than the bare membranes at all TMPs tested. Notably, we observed no signs of liquid-layer failure (i.e., complete removal of oil) even when testing was conducted at 4 bar TMP or after 10 cycles of use. While a small amount of the lower-viscosity Krytox 103 oil was removed during an initial pure water permeance test conducted at 1.5 bar TMP, we suggest that K103-LIMs can be pretreated by performing forward flushing or washing to remove this excess oil. No loss of K107 was quantified from the LIMs during our TGA analysis. In our static antifouling tests, LIMs demonstrated a ~50% improvement in fouling resistance over the bare membranes. While we acknowledge that future antifouling experiments should be conducted using long-term dynamic tests, this was beyond the scope of this work. Here, our goal was to provide the initial demonstration that multiple pure water permeance experiments could be conducted without the loss of the immobilized oil; our characterization of the membranes, including TGA data, staining, pure water permeance data, and strong antifouling results, demonstrates the retention of oil up to 10 cycles of membrane use, which was the most cycles that we tested due to the significant time required to conduct these tests. Future work in the area of LIMs could focus on broadening their applications via base membrane or oil selection. It may be possible to use low-tech support layers (i.e., coffee filters, fabrics) and/or edible immobilized layers 55,56 that could be purchased in a local convenience store. This work demonstrates that there is potential to reduce cleaning costs in membrane-based technologies thereby reducing the overall costs and improving the membrane lifetime.

ASSOCIATED CONTENT

Supporting Information

The Supporting Information is available free of charge at https://pubs.acs.org/doi/10.1021/acsami.1c20674.

Digital images of stained membranes, contact angle measurements, normalized permeance values, and TGA data are provided (PDF)

AUTHOR INFORMATION

Corresponding Author

Jessica D. Schiffman – Department of Chemical Engineering, University of Massachusetts Amherst, Amherst, Massachusetts 01003-9303, United States; orcid.org/0000-0002-1265-5392; Email: schiffman@umass.edu

Authors

- Rushabh M. Shah Department of Chemical Engineering, University of Massachusetts Amherst, Amherst, Massachusetts 01003-9303, United States
- Aydın Cihanoğlu Department of Chemical Engineering, University of Massachusetts Amherst, Amherst, Massachusetts 01003-9303, United States; orcid.org/0000-0003-3401-2416
- Justin Hardcastle Department of Chemical and Biomedical Engineering, University of Maine, Orono, Maine 04469, United States; Graduate School of Biomedical Science and Engineering, University of Maine, Orono, Maine 04469, United States
- Caitlin Howell Department of Chemical and Biomedical Engineering, University of Maine, Orono, Maine 04469, United States; Graduate School of Biomedical Science and Engineering, University of Maine, Orono, Maine 04469, United States; orcid.org/0000-0002-9345-6642

Complete contact information is available at: https://pubs.acs.org/10.1021/acsami.1c20674

Notes

The authors declare no competing financial interest.

ACKNOWLEDGMENTS

We thank Dr. Alexander Ribbe for experimental guidance with VP-SEM. R.M.S. thanks the American Membrane Technology Association (AMTA) and the United States Bureau of Reclamation for the Fellowship in Membrane Technology. A.C. was supported financially by the Scientific and Technological Research Council of Turkey (TÜBİTAK). The authors acknowledge the support of the National Science Foundation (award numbers 1930610 and 1930710).

REFERENCES

- (1) World Economic Forum. 2.2 billion people still don't have access to clean drinking water; https://www.weforum.org/agenda/2019/06/hotspots-h2o-new-un-report-details-global-progress-and-problems-with-access-to-safe-water-and-sanitation/ (accessed March 18, 2020).
- (2) UNICEF and WHO. 1 in 3 people globally do not have access to safe drinking water UNICEF, WHO; https://www.who.int/news-room/detail/18-06-2019-1-in-3-people-globally-do-not-have-access-to-safe-drinking-water-unicef-who (accessed March 18, 2020).
- (3) The Global Risks Report 2019; World Economic Forum: Geneva, Switzerland, 2019.
- (4) CDC. Global Diarrhea Burden; https://www.cdc.gov/healthywater/global/diarrhea-burden.html (accessed March 14, 2020)
- (5) Victora, C. G.; Wagstaff, A.; Schellenberg, J. A.; Gwatkin, D.; Claeson, M.; Habicht, J.-P. Applying an Equity Lens to Child Health and Mortality: More of the Same Is Not Enough. *Lancet* **2003**, *362*, 233–241.
- (6) Black, R. E.; Morris, S. S.; Bryce, J. Where and Why Are 10 Million Children Dying Every Year? *Lancet* 2003, 361, 2226–2234.
- (7) Boschi-Pinto, C. Estimating Child Mortality Due to Diarrhoea in Developing Countries. *Bull. World Health Organ.* **2008**, *86*, 710–717.

- (8) Stoller, M.; Baiocco, D.; Cicci, A.; Bravi, M. Description of the Biofouling Phenomena Affecting Membranes by the Boundary Flux Concept. *Chem. Eng. Trans.* **2016**, *49*, 589–594.
- (9) Dobosz, K. M.; Kolewe, K. W.; Schiffman, J. D. Green Materials Science and Engineering Reduces Biofouling: Approaches for Medical and Membrane-Based Technologies. *Front. Microbiol.* **2015**, *6*, No. 196
- (10) Belfort, G. Fluid Mechanics in Membrane Filtration: Recent Developments. *J. Membr. Sci.* **1989**, *40*, 123–147.
- (11) Du, X.; Wang, Y.; Leslie, G.; Li, G.; Liang, H. Shear Stress in a Pressure-Driven Membrane System and Its Impact on Membrane Fouling from a Hydrodynamic Condition Perspective: A Review. *J. Chem. Technol. Biotechnol.* **2017**, *92*, 463–478.
- (12) Cui, Z. F.; Wright, K. I. T. Flux Enhancements with Gas Sparging in Downwards Crossflow Ultrafiltration: Performance and Mechanism. *J. Membr. Sci.* **1996**, *117*, 109–116.
- (13) Laorko, A.; Li, Z.; Tongchitpakdee, S.; Youravong, W. Effect of Gas Sparging on Flux Enhancement and Phytochemical Properties of Clarified Pineapple Juice by Microfiltration. *Sep. Purif. Technol.* **2011**, *80*, 445–451.
- (14) Liang, H.; Gong, W.; Li, G. Performance Evaluation of Water Treatment Ultrafiltration Pilot Plants Treating Algae-Rich Reservoir Water. *Desalination* **2008**, 221, 345–350.
- (15) Samantaray, P. K.; Kumar, S.; Bose, S. 'Polycation' Modified PVDF Based Antibacterial and Antifouling Membranes and 'Point-of-Use Supports' for Sustainable and Effective Water Decontamination. *J. Water Process Eng.* **2020**, *38*, No. 101536.
- (16) Baker, J. S.; Dudley, L. Y. Biofouling in Membrane Systems A Review. *Desalination* **1998**, *118*, 81–89.
- (17) Mansouri, J.; Harrisson, S.; Chen, V. Strategies for Controlling Biofouling in Membrane Filtration Systems: Challenges and Opportunities. *J. Mater. Chem.* **2010**, *20*, 4567–4586.
- (18) Nafti Mateur, M.; Gonzalez Ortiz, D.; Jellouli Ennigrou, D.; Horchani-Naifer, K.; Bechelany, M.; Miele, P.; Pochat-Bohatier, C. Porous Gelatin Membranes Obtained from Pickering Emulsions Stabilized with H-BNNS: Application for Polyelectrolyte-Enhanced Ultrafiltration. *Membranes* 2020, 10, No. 144.
- (19) Zhou, W.; Fang, Y.; Li, P.; Yan, L.; Fan, X.; Wang, Z.; Zhang, W.; Liu, H. Ampholytic Chitosan/Alginate Composite Nanofibrous Membranes with Super Anti-Crude Oil-Fouling Behavior and Multifunctional Oil/Water Separation Properties. *ACS Sustainable Chem. Eng.* **2019**, *7*, 15463–15470.
- (20) Van Houdt, R.; Michiels, C. W. Biofilm Formation and the Food Industry, a Focus on the Bacterial Outer Surface. *J. Appl. Microbiol.* **2010**, *109*, 1117–1131.
- (21) Cappitelli, F.; Polo, A.; Villa, F. Biofilm Formation in Food Processing Environments Is Still Poorly Understood and Controlled. *Food Eng. Rev.* **2014**, *6*, 29–42.
- (22) Fang, L.-F.; Zhu, B.-K.; Zhu, L.-P.; Matsuyama, H.; Zhao, S. Structures and Antifouling Properties of Polyvinyl Chloride/Poly-(Methyl Methacrylate)-Graft-Poly(Ethylene Glycol) Blend Membranes Formed in Different Coagulation Media. *J. Membr. Sci.* 2017, 524, 235–244.
- (23) Xu, J.; Feng, X.; Hou, J.; Wang, X.; Shan, B.; Yu, L.; Gao, C. Preparation and Characterization of a Novel Polysulfone UF Membrane Using a Copolymer with Capsaicin-Mimic Moieties for Improved Anti-Fouling Properties. *J. Membr. Sci.* 2013, 446, 171–180.
- (24) Taurozzi, J. S.; Arul, H.; Bosak, V. Z.; Burban, A. F.; Voice, T. C.; Bruening, M. L.; Tarabara, V. V. Effect of Filler Incorporation Route on the Properties of Polysulfone—Silver Nanocomposite Membranes of Different Porosities. *J. Membr. Sci.* **2008**, 325, 58—68.
- (25) Bodner, E. J.; Kandiyote, N. S.; Lutskiy, M.-Y.; Albada, H. B.; Metzler-Nolte, N.; Uhl, W.; Kasher, R.; Arnusch, C. J. Attachment of Antimicrobial Peptides to Reverse Osmosis Membranes by Cu(I)-Catalyzed 1,3-Dipolar Alkyne—Azide Cycloaddition. *RSC Adv.* **2016**, *6*, 91815—91823.
- (26) Akar, N.; Asar, B.; Dizge, N.; Koyuncu, I. Investigation of Characterization and Biofouling Properties of PES Membrane

- Containing Selenium and Copper Nanoparticles. J. Membr. Sci. 2013, 437, 216–226.
- (27) Tiraferri, A.; Yip, N. Y.; Phillip, W. A.; Schiffman, J. D.; Elimelech, M. Relating Performance of Thin-Film Composite Forward Osmosis Membranes to Support Layer Formation and Structure. J. Membr. Sci. 2011, 367, 340–352.
- (28) Yang, X.; Du, Y.; Zhang, X.; He, A.; Xu, Z.-K. Nanofiltration Membrane with a Mussel-Inspired Interlayer for Improved Permeation Performance. *Langmuir* **2017**, *33*, 2318–2324.
- (29) Leng, C.; Sun, S.; Zhang, K.; Jiang, S.; Chen, Z. Molecular Level Studies on Interfacial Hydration of Zwitterionic and Other Antifouling Polymers in Situ. *Acta Biomater.* **2016**, *40*, 6–15.
- (30) He, M.; Gao, K.; Zhou, L.; Jiao, Z.; Wu, M.; Cao, J.; You, X.; Cai, Z.; Su, Y.; Jiang, Z. Zwitterionic Materials for Antifouling Membrane Surface Construction. *Acta Biomater.* **2016**, *40*, 142–152.
- (31) Nayak, K.; Kumar, A.; Das, P.; Tripathi, B. P. Amphiphilic Antifouling Membranes by Polydopamine Mediated Molecular Grafting for Water Purification and Oil/Water Separation. *J. Membr. Sci.* **2021**, *630*, No. 119306.
- (32) Ansari, A.; Peña-Bahamonde, J.; Wang, M.; Shaffer, D. L.; Hu, Y.; Rodrigues, D. F. Polyacrylic Acid-Brushes Tethered to Graphene Oxide Membrane Coating for Scaling and Biofouling Mitigation on Reverse Osmosis Membranes. J. Membr. Sci. 2021, 630, No. 119308.
- (33) Oshiba, Y.; Harada, Y.; Yamaguchi, T. Precise Surface Modification of Porous Membranes with Well-Defined Zwitterionic Polymer for Antifouling Applications. *J. Membr. Sci.* **2021**, *619*, No. 118772.
- (34) Miller, D. J.; Dreyer, D. R.; Bielawski, C. W.; Paul, D. R.; Freeman, B. D. Surface Modification of Water Purification Membranes. *Angew. Chem., Int. Ed.* **2017**, *56*, 4662–4711.
- (35) Venault, A.; Wei, T.-C.; Shih, H.-L.; Yeh, C.-C.; Chinnathambi, A.; Alharbi, S. A.; Carretier, S.; Aimar, P.; Lai, J.-Y.; Chang, Y. Antifouling Pseudo-Zwitterionic Poly(Vinylidene Fluoride) Membranes with Efficient Mixed-Charge Surface Grafting via Glow Dielectric Barrier Discharge Plasma-Induced Copolymerization. *J. Membr. Sci.* 2016, 516, 13–25.
- (36) Bohn, H. F.; Federle, W. Insect Aquaplaning: Nepenthes Pitcher Plants Capture Prey with the Peristome, a Fully Wettable Water-Lubricated Anisotropic Surface. *Proc. Natl. Acad. Sci. U.S.A.* **2004**, *101*, 14138–14143.
- (37) Wong, T.-S.; Kang, S. H.; Tang, S. K. Y.; Smythe, E. J.; Hatton, B. D.; Grinthal, A.; Aizenberg, J. Bioinspired Self-Repairing Slippery Surfaces with Pressure-Stable Omniphobicity. *Nature* **2011**, 477, 443–447.
- (38) Leslie, D. C.; Waterhouse, A.; Berthet, J. B.; Valentin, T. M.; Watters, A. L.; Jain, A.; Kim, P.; Hatton, B. D.; Nedder, A.; Donovan, K.; Super, E. H.; Howell, C.; Johnson, C. P.; Vu, T. L.; Bolgen, D. E.; Rifai, S.; Hansen, A. R.; Aizenberg, M.; Super, M.; Aizenberg, J.; Ingber, D. E. A Bioinspired Omniphobic Surface Coating on Medical Devices Prevents Thrombosis and Biofouling. *Nat. Biotechnol.* **2014**, 32, 1134–1140.
- (39) Sunny, S.; Vogel, N.; Howell, C.; Vu, T. L.; Aizenberg, J. Lubricant-Infused Nanoparticulate Coatings Assembled by Layer-by-Layer Deposition. *Adv. Funct. Mater.* **2014**, 24, 6658–6667.
- (40) Sunny, S.; Cheng, G.; Daniel, D.; Lo, P.; Ochoa, S.; Howell, C.; Vogel, N.; Majid, A.; Aizenberg, J. Transparent Antifouling Material for Improved Operative Field Visibility in Endoscopy. *Proc. Natl. Acad. Sci. U.S.A.* **2016**, *113*, 11676–11681.
- (41) Epstein, A. K.; Wong, T.-S.; Belisle, R. A.; Boggs, E. M.; Aizenberg, J. Liquid-Infused Structured Surfaces with Exceptional Anti-Biofouling Performance. *Proc. Natl. Acad. Sci. U.S.A.* **2012**, *109*, 13182–13187.
- (42) MacCallum, N.; Howell, C.; Kim, P.; Sun, D.; Friedlander, R.; Ranisau, J.; Ahanotu, O.; Lin, J. J.; Vena, A.; Hatton, B.; Wong, T.-S.; Aizenberg, J. Liquid-Infused Silicone As a Biofouling-Free Medical Material. *ACS Biomater. Sci. Eng.* **2015**, *1*, 43–51.
- (43) Hou, X.; Hu, Y.; Grinthal, A.; Khan, M.; Aizenberg, J. Liquid-Based Gating Mechanism with Tunable Multiphase Selectivity and Antifouling Behaviour. *Nature* **2015**, *519*, 70–73.

- (44) Overton, J. C.; Weigang, A.; Howell, C. Passive Flux Recovery in Protein-Fouled Liquid-Gated Membranes. *J. Membr. Sci.* **2017**, *539*, 257–262.
- (45) Bazyar, H.; Lv, P.; Wood, J. A.; Porada, S.; Lohse, D.; Lammertink, R. G. H. Liquid-Liquid Displacement in Slippery Liquid-Infused Membranes (SLIMs). *Soft Matter* **2018**, *14*, 1780–1788.
- (46) Bazyar, H.; Xu, L.; Vries, H. J. de.; Porada, S.; H Lammertink, R. G. Application of Liquid-Infused Membranes to Mitigate Biofouling. *Environ. Sci. Water Res. Technol.* **2021**, *7*, 68–77.
- (47) Kurtz, I. S.; Sui, S.; Hao, X.; Huang, M.; Perry, S. L.; Schiffman, J. D. Bacteria-Resistant, Transparent, Free-Standing Films Prepared from Complex Coacervates. *ACS Appl. Bio Mater.* **2019**, *2*, 3926–3933.
- (48) Rasband, W. S.; ImageJ, U. S. National Institutes of Health, Bethesda, Maryland, USA, https://imagej.nih.gov/ij/, 1997-2018.
- (49) Dobosz, K. M.; Kuo-LeBlanc, C. A.; Emrick, T.; Schiffman, J. D. Antifouling Ultrafiltration Membranes with Retained Pore Size by Controlled Deposition of Zwitterionic Polymers and Poly(Ethylene Glycol). *Langmuir* **2019**, *35*, 1872–1881.
- (50) Griffin, B. J. Variable Pressure and Environmental Scanning Electron Microscopy; Humana Press: Totowa, NJ, 2007; pp 467-495.
- (51) Tanaka, N.; Kogo, T.; Hirai, N.; Ogawa, A.; Kanematsu, H.; Takahara, J.; Awazu, A.; Fujita, N.; Haruzono, Y.; Ichida, S.; Tanaka, Y. In-Situ Detection Based on the Biofilm Hydrophilicity for Environmental Biofilm Formation. *Sci. Rep.* **2019**, *9*, No. 8070.
- (52) Kujawa, J.; Guillen-Burrieza, E.; Arafat, H. A.; Kurzawa, M.; Wolan, A.; Kujawski, W. Raw Juice Concentration by Osmotic Membrane Distillation Process with Hydrophobic Polymeric Membranes. *Food Bioprocess Technol.* **2015**, *8*, 2146–2158.
- (53) Lv, C.; Yang, Ć.; Hao, P.; He, F.; Zheng, Q. Sliding of Water Droplets on Microstructured Hydrophobic Surfaces. *Langmuir* **2010**, 26, 8704–8708.
- (54) Daniel, D.; Mankin, M. N.; Belisle, R. A.; Wong, T.-S.; Aizenberg, J. Lubricant-Infused Micro/Nano-Structured Surfaces with Tunable Dynamic Omniphobicity at High Temperatures. *Appl. Phys. Lett.* **2013**, *102*, No. 231603.
- (55) Manabe, K.; Kyung, K.-H.; Shiratori, S. Biocompatible Slippery Fluid-Infused Films Composed of Chitosan and Alginate via Layer-by-Layer Self-Assembly and Their Antithrombogenicity. *ACS Appl. Mater. Interfaces* **2015**, *7*, 4763–4771.
- (56) Wang, W.; Lockwood, K.; Boyd, L. M.; Davidson, M. D.; Movafaghi, S.; Vahabi, H.; Khetani, S. R.; Kota, A. K. Superhydrophobic Coatings with Edible Materials. *ACS Appl. Mater. Interfaces* **2016**, *8*, 18664–18668.

Supporting Information

Liquid-Infused Membranes Exhibit Stable Flux and Fouling Resistance

Rushabh M. Shah¹, Aydın Cihanoğlu¹, Justin Hardcastle^{2,3}, Caitlin Howell^{2,3}, and Jessica D. Schiffman^{1*}

¹Department of Chemical Engineering, University of Massachusetts Amherst, Amherst, Massachusetts 01003-9303, United States

²Department of Chemical and Biomedical Engineering, University of Maine, Orono, Maine 04469, United States

³Graduate School of Biomedical Science and Engineering, University of Maine, Orono, Maine 04469, United States

*Corresponding author: Jessica D. Schiffman; Email: schiffman@umass.edu

Table S1. TGA data acquired on as-prepared LIMs and LIMs used in permeance experiments conducted at 1.5 bar TMP.

Membrane		Krytox (%)	Bare Membrane (%)	K/M Ratio [†]
K103-LIM	As-Prepared	44 ± 5	38 ± 6	1.197 ± 0.39
	After Cycle 1	23 ± 7	53 ± 7	0.445 ± 0.16
	After Cycle 2	19 ± 6	57 ± 6	0.338 ± 0.11
	After Cycle 3	19 ± 9	60 ± 8	0.338 ± 0.18
	After Cycle 4	22 ± 6	57 ± 7	0.399 ± 0.14
	After Cycle 5	22 ± 7	54 ± 5	0.404 ± 0.13
K107-LIM	As-Prepared	41 ± 6	51 ± 6	0.839 ± 0.22
	After Cycle 1	40 ± 3	51 ± 4	0.805 ± 0.07
	After Cycle 2	36 ± 6	49 ± 7	0.744 ± 0.09
	After Cycle 3	34 ± 3	46 ± 5	0.738 ± 0.05
	After Cycle 4	36 ± 4	49 ± 5	0.750 ± 0.07
	After Cycle 5	36 ± 6	49 ± 5	0.728 ± 0.09

[†] K/M ratio was calculated using **Equation 4**.

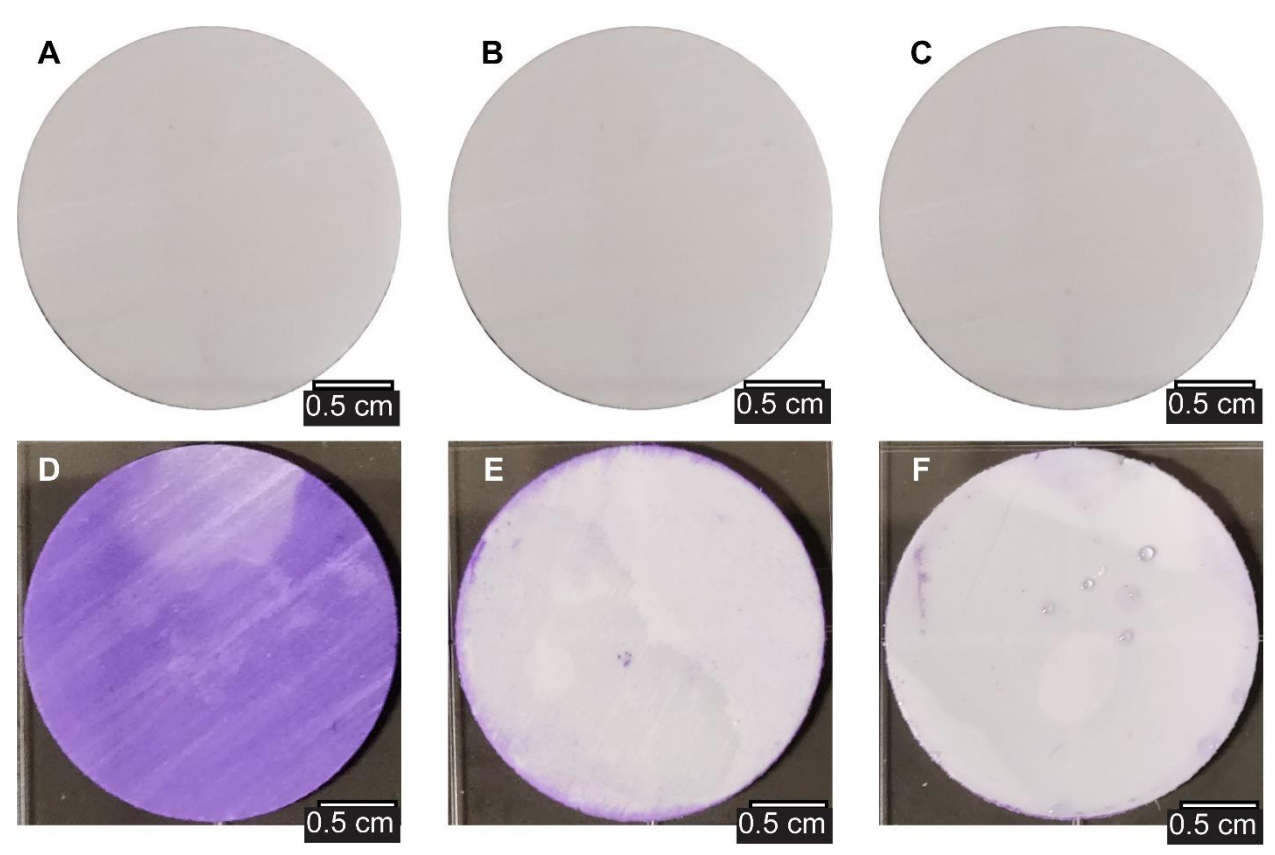


Figure S1. Digital images of (**A, D**) bare, (**B, E**) K103-LIMs and (**C, F**) K107-LIMs (top) before and (bottom) after staining with crystal violet. A 0.5 cm scale bar is provided.

Table S2. Contact angle measurements acquired on bare membranes.

Membrane	Static Contact Angle (°)	Tilt Contact Angle (°)
Bare	115 ± 8	> 45

Table S3. Contact angle measurements acquired on K103-LIMs and K107-LIMs.

Membrane	Tilt Contact Angle Post-Liquid Infusion (°)†	Tilt Contact Angle Post-60 min of vertical suspension (°)‡
K103-LIM	9 ± 4	37 ± 7*
K107-LIM	9 ± 3	19 ± 8*

[†]Post-liquid infusion implies that there may be excess oil on the surface

Table S4. Normalized permeance for K103-LIMs as a function of transmembrane pressure (TMP).

Applied Pressure (bar)	Normalized Permeance (PWP/PWP ₀)
1.0	0.01 ± 0.002
1.3	0.15 ± 0.08
1.5	0.28 ± 0.06
2.0	0.36 ±0.03

[‡]These fully prepared LIMs include the 60 min of vertical suspension post-liquid infusion; this is the full preparation method used throughout this study

^{*}Denotes a p ≤ 0.05 significance between samples

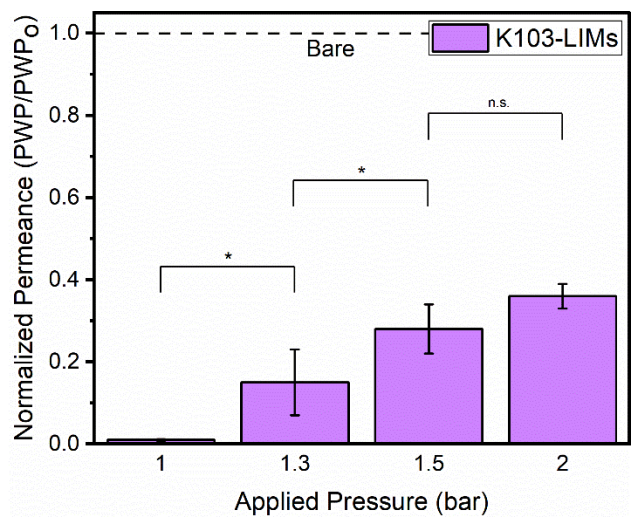


Figure S2. Normalized permeance for K103-LIMs as a function of transmembrane pressure (TMP). The dotted line represents the normalized permeance of the bare membranes. Error bars denote standard deviation, one asterisk (*) denotes a p \leq 0.05 significance between samples, and n.s. denotes that samples were not statistically different.

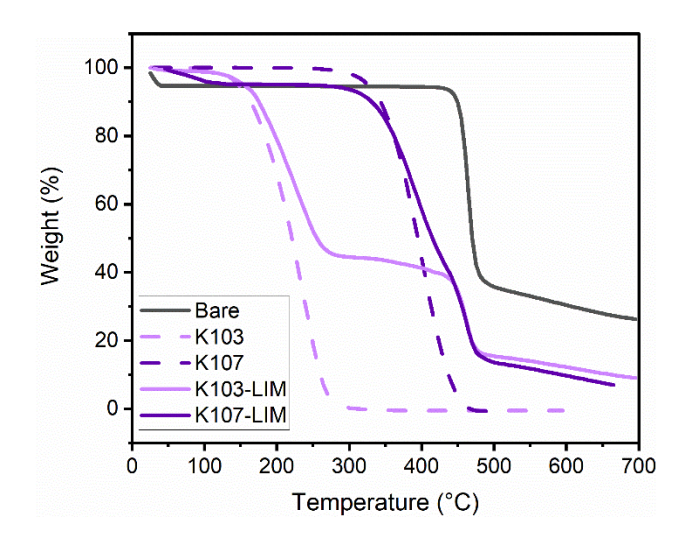


Figure S3. TGA data acquired on bare membranes, K103 and K107 lubricants, and asprepared K103-LIMs and K107-LIMs.